# An Elastic "Sieve" to Probe Momentum Space: Gd Chains on W(110)

O. Rader[1] and A. M. Shikin[1,2]

[1]*BESSY, Albert-Einstein-Strasse 15, D-12489 Berlin, Germany*

[2]*Institute of Physics, St. Petersburg State University, St. Petersburg 198904, Russia*

(Received 29 May 2004; published 13 December 2004)

Electron scattering conditions of one-dimensional nanostructures are explored in angle-resolved photoelectron spectroscopy. Tiny increments of the Gd submonolayer coverage on W(110) lead to strong modifications in the spectra. It is shown that the Gd overlayer represents an elastic superlattice of chains which performs a systematic mapping of the electronic band dispersion of the W substrate through a quasicontinuous series of umklapp wave vectors. Conversely, a single valence-band spectrum contains essential and precise structural information readily accessible by comparison to the band dispersion.

DOI: 10.1103/PhysRevLett.93.256802 PACS numbers: 73.21.Fg, 71.20.Eh, 79.60.–i

Our knowledge of the electronic structure of solids is largely based on measurements by angle-resolved photoelectron spectroscopy since it is the only method to deliver $E(\mathbf{k})$ band dispersions of the valence electrons [1]. These band dispersions determine many fundamental properties like electrical conductivity, magnetism, optical properties, and mechanical properties along the various crystallographic directions, and numerous data have meanwhile been measured and compiled [2]. In order to perform a band mapping experiment on a crystal, it has been necessary to either exploit the conservation of the electron momentum parallel to the surface $\mathbf{k}_{\parallel}$ by measuring different emission angles of the photoelectron or change the wavelength of the exciting photon source to vary the perpendicular wave vector $\mathbf{k}_{\perp}$ along a high symmetry direction of the crystal [1].

With the exploration of the properties of ultrathin films as two-dimensional quantum-well structures, another method to determine $E(\mathbf{k})$ has been devised [3]. It was realized that the interface between the film and the crystalline substrate on which it is grown can serve as a sufficient scatterer for electrons to lead to electron confinement similar as with light waves in an optical Fabry-Perot interferometer. This allows a most precise mapping of the band dispersion by just varying the film thickness layer by layer in an angle-resolved photoelectron spectroscopy experiment [4].

The recent quest for lateral electron confinement in one-dimensional nanostructures has led to impressive interference effects of electron waves when atomic barriers are artificially constructed with the tip of a scanning tunneling microscope (STM) [5] or at the step edges at miscut crystal surfaces as natural scatterers [6]. We therefore pose the question whether lateral nanostructures can offer yet another way to experimentally obtain a band dispersion by photoelectron spectroscopy. To this end, a superlattice of scatterers needs to be constructed with the possibility to tune its lattice constant $d$ over a considerable range. This superlattice could act like a "sieve" selecting the electron momentum $k$ according to $k = 2\pi/d$. It appears promising to utilize self-organization tendencies among adatoms with repulsive interactions and to break the symmetry by a substrate with a rectangular unit cell in order to force the atoms into chains. Au atoms on Ni(110) form such repulsive chains with a perfect one-dimensional electronic structure but the system has a complicated geometry since the Au is partially immersed in the Ni surface layer [7].

Enhanced versatility is expected turning to adsorbates with stronger repulsive interactions. Adsorbed rare-earth atoms on W(110) experience charge transfer which results in the formation of a strong atomic dipole perpendicular to the surface. The repulsive dipole-dipole interaction among the rare-earth atoms stabilizes a series of superstructures at room temperature [8,9]. Figure 1 displays the structures realized below 0.7 monatomic layers (ML) Gd/W(110) following the characterization by low-energy electron diffraction (LEED) and STM in Refs. [8,9]: Although the $10 \times 2$ structure at lowest coverage is a rectangular surface lattice, it is better described as chains running along the $[1\bar{1}0]$ direction of the W(110) substrate.

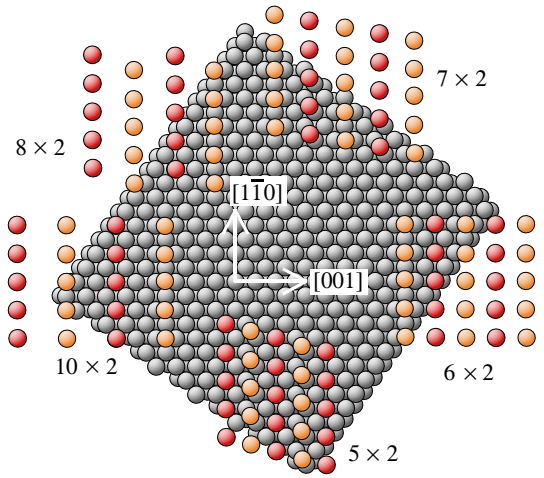


FIG. 1 (color online). Structure of Gd on W(110). Chains along $[1\bar{1}0]$ are formed which approach each other for increased Gd deposition. Colors mark Gd atoms with relatively higher (red) and lower (orange) positions according to Ref. [9].

 

With increasing coverage, more Gd atoms need to be squeezed in and are accommodated in new oblique lattices in which the chains successively approach each other along [001]. The interatomic distance along the chains is thereby conserved.

The experiment has been performed using a hemispherical photoelectron analyzer with 1° angle resolution and linearly polarized synchrotron light from undulator beam lines U125/1 PGM and UE56/1 PGM at BESSY [10]. Preparation of the W(110) sample and deposition of Gd have been done as described in Ref. [11] for thicker Gd/W(110).

Figure 2 shows at the bottom the clean W(110) spectrum characterized by W 6*s* states at −6.3 eV and intense emission from a W 5*d* surface resonance around −1.2 eV (0 eV corresponds to the Fermi energy $E_F$) [12]. Along the [110] surface normal, W(110) displays an even-symmetry bulk band gap extending from −2 to −6.3 eV [12]. For a photon energy of 62.5 eV, direct transitions from the lower boundary of this gap (−6.3 eV at the *N* point of the Brillouin zone) dominate the spectrum. Gd was deposited onto the W(110) substrate at room temperature, and after each deposition step the sample was annealed to ~250 °C for 2 min. The first indication of Gd adsorption is from the unresolved multiplet of Gd 4*f* emission ($4f^6$ final state) at −8.3 eV and 0.28 ML coverage. While the W surface resonance and the W 6*s* peak have lost intensity, new shoulders appear at −5.4 and −2.3 eV for 0.28 ML. At 0.39 ML, one shoulder has moved to −4.7 eV, and with each further Gd deposition step, the spectral shape changes continuously and becomes dominated by the new features. This behavior, unprecedented in submonolayer growth, continues until the spectral shape saturates with the completion of the first Gd monolayer indicated most clearly by a shift of the Gd 4*f* levels from −8.3 to −8.05 eV.

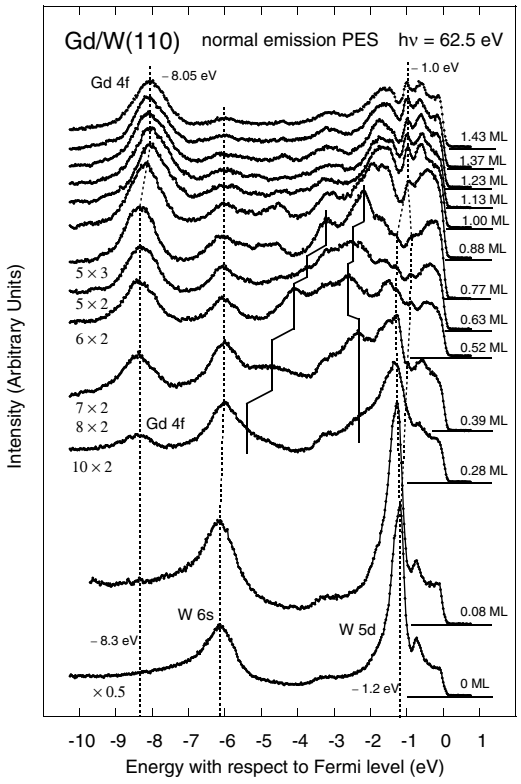


FIG. 2. Photoemission spectra of the valence band for various Gd coverages on W(110). In the range of the forbidden gap of W (− 2.0 to −6.3 eV) strong changes occur.

Before connecting the observed behavior to the series of superstructures shown in Fig. 1, we perform a test on the origin of the new photoemission structures. As direct photoemission transitions from W are symmetry forbidden in the energy range −2 to −6.3 eV (the small shoulder at −3.3 eV is a so-called high density-of-states peak), emission from Gd 5*d* states is a possible cause for the new features. Resonant photoemission at the Gd 4*d* excitation threshold (maximum at ~149 eV photon energy) can unambiguously distinguish Gd- from W-derived valence-band states. The resonance process enhances very strongly the Gd 4*f* emission via $4d^{10}4f^7 + h\nu \rightarrow 4d^9 4f^8 \rightarrow 4d^{10}4f^6 + e^-$ but at the same time also the Gd 5*d* emission via $4d^{10}4f^7 5d^n + h\nu \rightarrow 4d^9 4f^8 5d^n \rightarrow 4d^{10}4f^7 5d^{n-1} + e^-$. In Fig. 3, the Gd deposition was repeated without annealing and besides 62 eV two vicinal photon energies, 145 and 147 eV, were used. Between these energies the resonant photoemission intensity rises steeply so that the area enclosed between 147 and 145 eV spectra can be taken as a good approximation of the Gd 5*d* density of states. Interestingly, on this basis none of the peaks in the forbidden gap can be assigned to Gd which rather appears in the energy range between −2 eV and $E_F$. All new structures marked in Fig. 2 are therefore derived from W.

The behavior of the spectra in Fig. 2 bears a certain similarity to $E(\mathbf{k})$ band dispersions but with *k* replaced by the Gd coverage. The connection to the superstructures of Gd chains is explained in Fig. 4(a) which shows a cross section through the $(1\bar{1}0)$ plane of the crystal in reciprocal space. It is identical to the Ewald construction for LEED but taking the photoelectron as the primary wave. $\bar{\Gamma}$ is the center of the first surface Brillouin zone of W(110), identified with normal electron emission, and represented by a rod perpendicular to the surface plane. $\bar{\Gamma}'$ is the center of the second surface Brillouin zone of W(110), separated by 4.0 $\text{Å}^{-1}$ along [001]. In addition, reciprocal lattice rods (dashed) from an arbitrary superstructure are shown. All these rods correspond to centers of the superlattice Brillouin zone and one point on a rod away from $\bar{\Gamma}$ is chosen. Figure 4(a) indicates how this point, $\mathbf{k}_{i,1}$, can nevertheless contribute to normal electron emission ($\bar{\Gamma}$) through a single scattering event at the superlattice or surface reconstruction. This is represented by the diffraction vector $\mathbf{G}_1$ on the Ewald sphere. In angle-resolved photoelectron spectroscopy, this is a nondirect transition known as the umklapp process [13]: $\mathbf{k}_{\parallel}$ is

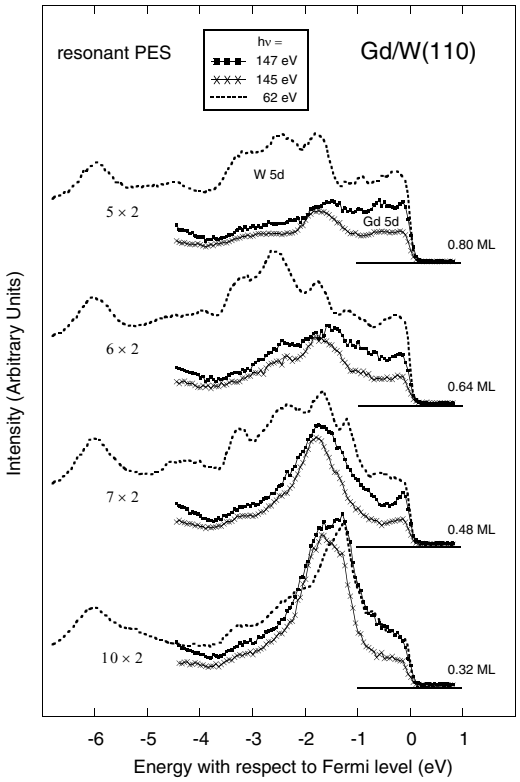


FIG. 3. Photoemission spectra at 62 eV photon energy as compared to resonant photoemission spectra. The difference between resonant photoemission spectra at 147 and 145 eV corresponds to the Gd 5*d* density-of states. All characteristic features seen at 62 eV are derived from W.

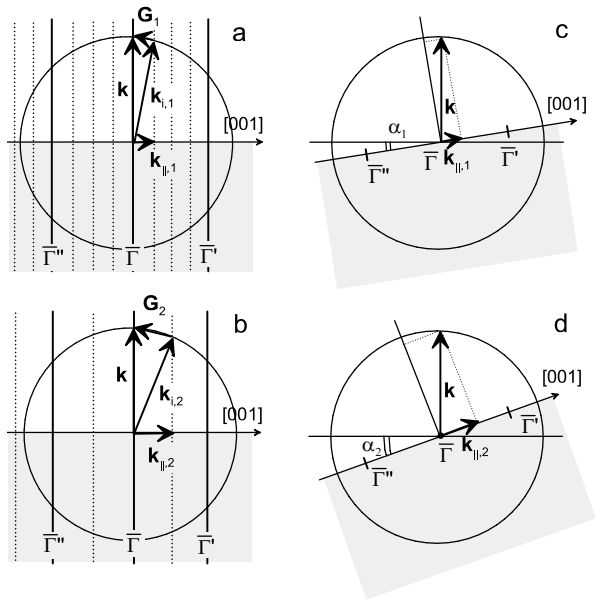


FIG. 4. Proposed model. Reciprocal lattice rods for the W(110) surface (solid vertical lines) and for a Gd superlattice (dotted lines) (a). W bulk states away from $\overline{\Gamma}$ can contribute to normal-emission spectra via a diffraction vector $\mathbf{G}_1$. For the given system, the parallel component $\mathbf{G}_\parallel = -\mathbf{k}_\parallel$ increases in proportion with the adsorbate coverage (b). For comparison, angle-dependent photoemission obeys the same relationships between $\mathbf{k}$ and $\mathbf{k}_\parallel$ when the emission angle $\alpha$ is varied thus probing the same initial states in the bulk Brillouin zone of W (c),(d).

conserved when the electron passes through the surface according to $\mathbf{k}_\parallel^{\text{ext}} = \mathbf{k}_\parallel^{\text{int}} + \mathbf{G}_\parallel$ where $\mathbf{G}_\parallel$ represents any reciprocal lattice vector in the surface plane. This relationship has been used to assign unexpected features in photoemission spectra but never systematically or without varying $\mathbf{k}_\perp$ [13]. For the present experiment, this means that the $10 \times 2$ structure corresponds to $\mathbf{k}_\parallel = -\mathbf{G}_\parallel = \frac{1}{10}\overline{\Gamma\Gamma}'$ or 0.40 Å$^{-1}$. Figure 4(b) shows how $\mathbf{k}_\parallel$ increases with increasing Gd coverage as the $n \times 2$ series continues with 0.50 Å$^{-1}$ ($8 \times 2$), 0.57 Å$^{-1}$ ($7 \times 2$), 0.66 Å$^{-1}$ ($6 \times 2$), and 0.80 Å$^{-1}$ ($5 \times 2$) along [001]. The umklapp vector $\mathbf{k}_\parallel$ although given by the Gd probes momentum space of the W.

The validity of this interpretation can directly be checked in the experiment. The basis is the observation that angle-dependent photoemission is governed by the same relationships as the umklapp effect: In angle-dependent photoemission, Figs. 4(c) and 4(d), the sample is tilted off normal against the detector by an angle $\alpha$ giving the electron wave vector that is probed a parallel component $|\mathbf{k}_\parallel| = (\sqrt{2mE_{\text{kin,vac}}}/\hbar)\sin\alpha$. The Ewald spheres in Fig. 4 indicate further that any identity $\mathbf{G}_1 = \mathbf{k}_{\parallel,1}$ determines that also the respective perpendicular components $\mathbf{k}_\perp$ are equal (neglecting changes of the work function); i.e., the same point of the bulk Brillouin zone is sampled in 4(a) and 4(c) and in 4(b) and 4(d), respectively.

As a demonstration, we show in Fig. 5(a) a Gd coverage dependence measured under the same conditions as in Figs. 2 and 3 but at room temperature and smaller coverage steps of ~0.03 ML and displayed in a color representation *vis à vis* the angle dependence for clean W(110) along [001]. For a Gd coverage from 0 up to ~0.7 ML, where the intrachain distance remains constant, an impressive similarity between the two cases is observed in the energy range of the gap (− 2.0 to −6.3 eV). The fact that the $\mathbf{k}_\parallel$ vector does not change continuously but in discrete steps can be seen from the strongly dispersing band in Fig. 5(a). Energies jump rather abruptly from −4.1, −4.6, to −5.4 eV in a range where the Gd coverage is varied in 10 steps at least.

A few remarks should be made concerning the implications of these results. The results emphasize the importance of electron scattering and demonstrate that it will seriously complicate the interpretation of electron spectroscopy of nanostructures assembled on flat, prepatterened, or stepped substrates. The effect occurs more strongly the better the nanostructures are ordered. The present results represent, on the other hand, only the starting point of a more systematic exploitation of the structural information contained in the umklapp emis-

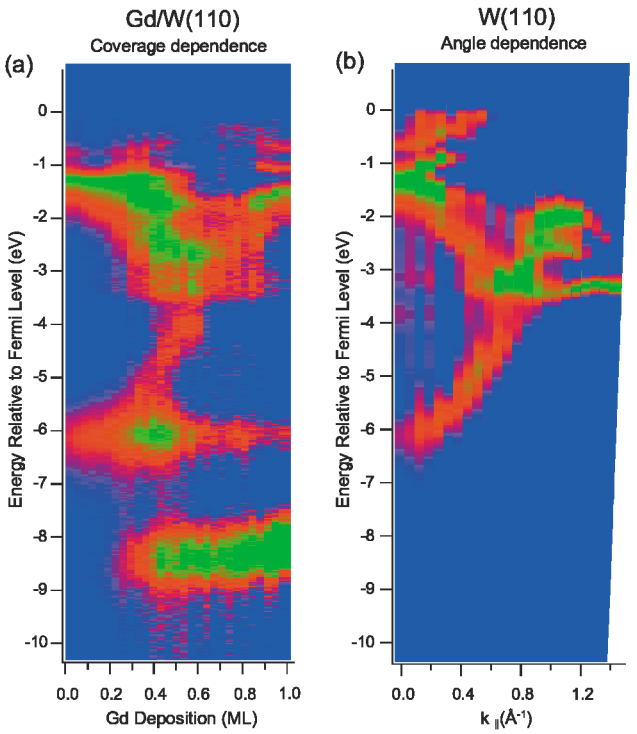


FIG. 5 (color). Coverage dependence in normal emission of Gd/W(110) (a) versus emission angle dependence of clean W(110) along [001] (b). The Gd overlayer provides for a quasicontinuous series of umklapp vectors $\mathbf{G}_{\parallel}$ in proportion to the Gd coverage to sample the W bulk band structure. Up to ~0.8 ML, all transitions inside of the gap (−2 to −6.3 eV) are of the umklapp type. Note the direct transitions at −6.3 eV (N-point of W) and −8.3 eV (Gd 4*f*).

sion. The structural information contained in the umklapp-induced peaks can indeed serve as the basis of a coverage calibration of unprecedented precision and can be used to assign the initial-state effects simultaneously present in the spectra. We want to briefly return to Fig. 2 to point out the behavior of the W surface resonance at −1.2 eV. It was found that this surface resonance directly connects to the two-dimensional Fermi surface of W(110) [14]. The changes of the surface resonance observed in Fig. 2 indicate that Gd acts on the Fermi surface. The dipole interaction between Gd atoms is basically isotropic, but using the structural information contained in the umklapp part of an individual valence-band spectrum together with electronic properties from the direct transitions, it will be possible to identify the modifications of the Fermi surface which force the Gd atoms into chains and in this way put the geometry down to the electronic structure.

In summary, we have shown how a coherent array of Gd nanostructures, stable at room temperature on W(110), can be used to probe the electronic structure of the W substrate through a series of nondiret photoemission transitions. This emphasizes in an impressive way the importance of scattering when studying electronic properties, and some resulting problems and perspectives for nanostructure research have been addressed.

We acknowledge participation of C. Pampuch, G.V. Prudnikova, and A. Varykhalov in parts of the experiment and thank R. Follath for expert support with the U125 beam line. This work was supported by DFG (RA 1041/1-1 and 436RUS113/735/0-1), the common DFG-RFFI project (03-02-04-024), and the Russian program "Surface and Atomic Structures."

[1] *Angle Resolved Photoemission*, edited by S. D. Kevan (Elsevier, Amsterdam, 1992); S. Hüfner, *Photoelectron Spectroscopy* (Springer, Berlin, 1995).
[2] *Electronic Structure of Solids: Photoemission Spectra and Related Data*, edited by A. Goldmann, Landolt-Börnstein, New Series, Group III, Vol. 23 (Springer, Berlin, 1999).
[3] R. C. Jaklevic and J. Lambe, Phys. Rev. Lett. **26**, 88 (1971); P. D. Loly and J. B. Pendry, J. Phys. C **16**, 423 (1983).
[4] J. J. Paggel, T. Miller, and T. C. Chiang, Science **283**, 1709 (1999); T. C. Chiang, Surf. Sci. Rep. **39**, 181 (2000).
[5] M. F. Crommie, C. P. Lutz, and D. M. Eigler, Science **262**, 218 (1993).
[6] P. Avouris and I.W. Lyo, Science **264**, 942 (1994); L. Burgi, O. Jeandupeux, A. Hirstein, H. Brune, and K. Kern, Phys. Rev. Lett. **81**, 5370 (1998); A. Mugarza, A. Mascaraque, V. Perez-Dieste, V. Repain, S. Rousset, F. J. Garcia de Abajo, and J. E. Ortega, Phys. Rev. Lett. **87**, 107601 (2001).
[7] C. Pampuch, O. Rader, T. Kachel, W. Gudat, C. Carbone, R. Kläsges, G. Bihlmayer, S. Blügel, and W. Eberhardt, Phys. Rev. Lett. **85**, 2561 (2000).
[8] J. Kołaczkiewicz and E. Bauer, Surf. Sci. **175**, 487 (1986).
[9] R. Pascal, Ch. Zarnitz, M. Bode, and R. Wiesendanger, Phys. Rev. B **56**, 3636 (1997).
[10] R. Follath, F. Senf, and W. Gudat, J. Synchrotron Radiat. **5**, 769 (1998); M. R. Weiss *et al.*, Nucl. Instrum. Methods Phys. Res., Sect. A **467–468**, 449 (2001).
[11] O. Rader and A. M. Shikin, Phys. Rev. B **64**, 201406(R) (2001).
[12] R. H. Gaylord and S. D. Kevan, Phys. Rev. B **36**, R9337 (1987); J. Feydt, A. Elbe, H. Engelhard, G. Meister, Ch. Jung, and A. Goldmann, Phys. Rev. B **58**, 14 007 (1998).
[13] E. O. Kane, Phys. Rev. Lett. **12**, 97 (1964); J. Anderson and G. J. Lapeyre, Phys. Rev. Lett. **36**, 376 (1976); D. Westphal and A. Goldmann, Surf. Sci. **126**, 253 (1983); G. Paolucci, K. C. Prince, B. E. Hayden, P. J. Davie, and A. M. Bradshaw, Solid State Commun. **52**, 937 (1984).
[14] R. H. Gaylord, K. H. Jeong, and S. D. Kevan, Phys. Rev. Lett. **62**, 2036 (1989).